The following publication B. Zhou et al., "Optimal Coordination of Electric Vehicles for Virtual Power Plants With Dynamic Communication Spectrum Allocation," in IEEE Transactions on Industrial Informatics, vol. 17, no. 1, pp. 450-462, Jan. 2021 is available at https://doi.org/10.1109/TII.2020.2986883

Optimal Coordination of Electric Vehicles for Virtual Power Plants with Dynamic Communication Spectrum Allocation

Bin Zhou, *Senior Member, IEEE*, Kuan Zhang, Ka Wing Chan, *Member, IEEE*, Canbing Li, *Senior Member, IEEE*, Xi Lu, Siqi Bu, *Senior Member, IEEE*, Xiang Gao

***Abstract*—This paper proposes an optimal coordinated scheduling of electric vehicles (EVs) for a virtual power plant (VPP) considering communication reliability. Recent advancements on wireless technologies offer flexible communication solutions with wide coverage and low-cost deployment for smart grid. Nevertheless, the imperfect communication may deteriorate the monitoring and controlling performance of distributed energy resources. An interactive approach is presented for combined optimization of dynamic spectrum allocation and EV scheduling in the VPP to coordinate charging/discharging strategies of massive and dispersed EVs. In the proposed approach, a dynamic partitioning model of the multi-user multi-channel cognitive radio is used to cope with the vehicle-to-grid (V2G) communication issue due to variable EV parking behaviors, and a two-stage V2G dispatch scheme is proposed for the wind-solar-EV VPP to maximize its overall daily profit. Furthermore, the effects of packet loss probability on the VPP scheduling performance and battery degradation cost are thoroughly analyzed and investigated. Comparative studies have been implemented to demonstrate the superior performance of the proposed methodology under various imperfect communication conditions.**

***Index Terms*—Smart grid, vehicle to grid, stochastic optimization, virtual power plant, wireless communication.**

I. Introduction

Electric vehicles (EVs) are considered as an important means of stabilizing the smart grid and facilitating the integration of renewable energy through vehicle-to-grid (V2G) operation [1]. As an emerging energy storage form, EVs could feed the stored electricity back into power grids to provide energy services in a distributed manner when parked and connected to the grid [2]. It is reported in [3] that the global EV deployment would reach 20 million by 2020 and 140 million by 2030, while personal EVs are utilized only 4% of their time for transportation [4]. Hence, the EV fleets are potentially available to provide fast response and large battery storage capacity for V2G implementation, and can be aggregated and controlled under the virtual power plant (VPP) architecture to participate in energy markets [5]-[7].

The increasing number of EVs can enhance the V2G capability for energy arbitrage and peak shaving, and thus can decrease the initial investment for dedicated energy storage in the VPP [5]-[8]. Over the years, most of EVs adopt lead-acid and nickel-metal hydride batteries due to their mature technologies and low costs. Nevertheless, the ageing and degradation of batteries accelerates linearly or even exponentially with the increase of the depth of discharge (DOD) for these EV batteries, which is recognized as a main obstacle to the widespread implementation of V2G programs [9]. Nowadays, lithium-ion batteries have been extensively accepted by EV industries because of their exceptionally long cycle life and low battery degradation cost [3]. The techno-economic analysis of V2G feasibility has been studied in [2],[8],[10] that the commercial V2G hub are cost effective to cover the associated battery degradation cost via electricity price arbitrage, and lithium-ion batteries of EVs can achieve 5000 and 1,000,000 cycles at 70% and 3% DOD, respectively. Moreover, it is reported in [11] that 50 landmark V2G projects around the world, e.g., Parker Project and M-Tech Labo, have been successfully launched, contributing to improving the reliability and efficiency of smart grid with considerable economic benefits for both of power utilities and EV users. However, the available battery capacity from EVs usually varies over different hours of the day depending on mobility behaviors of EV owners [12], and thus the coordination and management of these geographically scattered EVs give rise to a challenge for V2G communication and control strategies [13]-[16].

The V2G operation requires a bidirectional grid-connected EV charger with metering and communication capabilities [16], and the coordinated scheduling of EVs involves information interactions among the VPP and chargers in real-time, such as the time of arrival/departure, battery state of charge (SOC) and real-time control signals [1]. So far, various studies have been reported in [15]-[19] to implement the V2G under the problem of imperfect data communication. The effects of availability, economics and reliability of a hierarchical communication architecture on V2G ancillary services were analyzed in [18],[19] and distributed methods were also presented in [15],[16] to investigate the V2G dispatch and communication strategies for EV aggregators. Most existing literatures have focused on the optimal V2G programs with small-scale EVs (e.g., less than 100 EVs), and the scalability of these strategies on the monitoring and controlling performance of numerous end-users (e.g., more than 1000 EVs) are not involved yet. Although the wired and wireless technologies of V2G communication are developing rapidly, it is difficult to guarantee a perfect two-way communication network for massive and scattered EVs due to the huge investment cost of high-bandwidth communication channels [17],[18]. Consequently, this inevitably leads to the performance degradation of the price-responsive VPP dispatch under an imperfect communication network [19].

Wireless technologies have been widely recognized for smart grid communications due to their widespread access and low-cost deployment [20], especially for demand response and V2G systems [21]. As the information exchange among the VPP control center and numerous decentralized EVs should be communicated within a limited time period for real-time V2G operation, significant spectrum resources are thus required due to the large

This work was jointly supported by the National Natural Science Foundation of China (51877072) and Huxiang Young Talents Programme of Hunan Province under Grant 2019RS2018. Paper no. TII-19-5424. *(Corresponding authors: Canbing Li; Ka Wing Chan.)*

B. Zhou, K. Zhang, and C. Li are with the College of Electrical and Information Engineering, Hunan University, Changsha 410082, China, and also with the Hunan Key Laboratory of Intelligent Information Analysis Integrated Optimization for Energy Internet, Hunan University, Changsha 410082, China (e-mail: binzhou@hnu.edu.cn; zhangkuan1994@qq.com; licanbing@qq.com).

K. W. Chan, X. Lu, S. Bu, and X. Gao are with the Department of Electrical Engineering, The Hong Kong Polytechnic University, Hong Kong. (e-mail: eekwchan@polyu.edu.hk; harry.lu@connect.polyu.hk; siqi.bu@gmail.com; jocelyn.gao@connect.polyu.hk).

volume of real-time data traffic for the monitoring and control of these EVs [22]. However, with the increasingly intensive radio systems operating in the license-free industrial, scientific, medical (ISM) frequency band (e.g., WiFi, Bluetooth and Zigbee), the wireless spectrum becomes remarkably crowded and insufficient over the limited ISM band [23]. Also, the cellular network can employ exclusively the licensed ultra-high-frequency bands to support long-range V2G systems, but these spectrum bands have already been completely allocated for specific uses, making it difficult to acquire dedicated spectra for the large-scale EV dispatch [24]. As a consequence, the available radio spectrum bandwidth for the real-time V2G communication appears to be gradually scarce in recent years, and therefore the investment and operation costs to lease new licensed spectrum bands for a large number of EVs would be expensive [25].

As reported from the U.S. Federal Communications Commission in [26], the allocated licensed spectrum is heavily under-utilized in the temporal and spectral dimensions. Cognitive radio (CR) is a promising technique to address this problem using dynamic spectrum access [22], and it can be incorporated in the existing V2G communication to satisfy the desire of large-scale EV applications [23]-[25]. With the aid of CR, the EVs can act as secondary users (SUs) to opportunistically operate in the vacant licensed spectrum bands from primary users (PUs) so as to improve the utilization of wireless spectrums. Recently, various CR channel partition schemes have been reported in [22]-[28] to effectively manage the spectrum resources of PUs among different SUs. Nevertheless, the communication performance would be adversely affected by the uncertainties of numerous SUs resulted from the mobility nature of EVs.

In order to improve the V2G communication and control performance with the uncertainty of the presence of EVs at charging stations, a V2G dispatch framework based on rolling horizon optimization (RHO) is proposed for the wind-solar-EV VPP to maximize its total profit under imperfect communication effects. The main contributions of this work are summarized as follows: 1) An interactive approach is proposed to dynamically optimize the CR spectrum allocation and EV charging/discharging strategy considering the variable number of EVs at charging stations; 2) A scenario-based rolling horizon strategy is presented to incorporate the renewable energy and EV uncertainties considering the packet loss of data metering; 3) The effects of data packet loss probability on the VPP performance and battery degradation cost are further analyzed and investigated. Comparative studies have not only demonstrated the superior performance of the proposed approach for V2G communication and dispatch, but also confirmed the improved VPP profit under various imperfect communication conditions.

II. Problem Formulation

A. VPP Architecture with CR network

As illustrated in Fig. 1, the VPP is composed of wind power plants (WPPs), photovoltaics (PVs) and EVs, and these distributed energy installations are collectively managed by a central control entity with the CR network [6],[24]. Both the day-ahead market and the balancing real-time market, operating at different time horizons, are involved to provide flexible energy trading for VPPs. In the day-ahead market, the VPP submits offers/bids for the day-ahead schedule of electricity trading, while the balancing market enables the VPP to sell or purchase electricity, in a near real time, for settling the energy imbalances caused by stochastic PV and WPP generations [29]. It is reported in [2],[4] that EVs will be parked at either work or home for a majority of the time, and the batteries only require to be charged with enough energy before their departure time. Hence, EVs can collectively serve as large-capacity energy storage to mitigate the volatility and intermittency of PV and WPP outputs, and facilitate the VPP to boost its total profit by moving electricity delivery through hours.

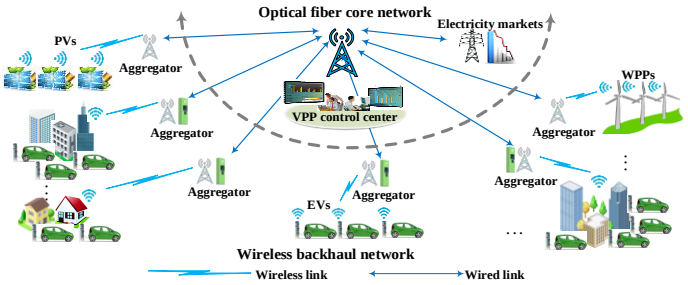

Fig. 1 Architecture of the VPP with CR network

As shown in Fig. 1, a hierarchical communication infrastructure with CR network is integrated into the VPP control center to offer secure and efficient access to large-scale distributed energy resources [23]. In this hierarchical architecture, the aggregators serve as the intermediary entity between the control center and a large number of EVs to implement the V2G dispatch. The core networks in the upper layer provide the wired connection to aggregators to guarantee high data reliability using the fiber-optic communication. In the wireless backhaul networks, each aggregator can be used as a cognitive node to communicate with the dispersed smart meters deployed in EV chargers and renewable energy sources (RESs). The CR technique can handle the broadband connection to wireless local area networks for monitoring EVs, and also contribute to decreasing the investment cost and enhancing the communication flexibility and coverage [25].

B. Real-time Monitoring and Communication Framework

During the VPP dispatch and communication process, a large amount of real-time data information exchange from smart meters is required, including SOC levels of EV batteries, EV-driving characteristics, the charging/discharging control signals to EVs, weather data as well as the power outputs of WPPs and PVs, etc. Since smart meters cannot perform the information monitoring and communication simultaneously, the collected data of EVs and RESs will be transmitted to the VPP control center in limited time durations [28]. Fig. 2 shows the real-time monitoring and communication framework of smart meters. It can be found that, each dispatch cycle time of VPP, T_{D}, consists of two phases: monitoring duration T_{m} and communication duration T_{c}. The T_{c} can further be divided into K time slots, and at most one data packet can be transmitted in a time slot [27]. However, the limited CR bandwidth and the finite communication duration cannot allow all of the metering data to be transmitted successfully, and thus the packet loss may be resulted, e.g., the metering data are considered to be lost once the data have not been transmitted within the communication duration.

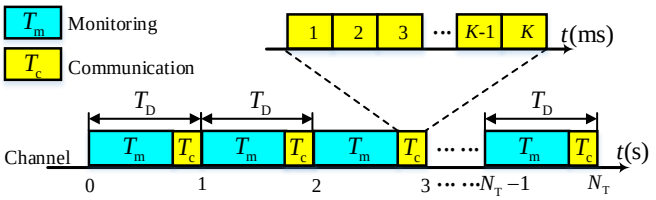

Fig. 2 Framework of a cycle time for real-time monitoring and communication

The real-time monitoring information from RESs and EVs, in combination with the weather and price data, is characterized to contain large volumes of multiple types of data. In contrast, the real-time charging/discharging control signal data from the VPP control center to each EV is characterized as small volumes and delay sensitive [24]. Since EV control signals are of great importance for the VPP dispatch performance, the automatic repeat request technique in [28] is used for wireless communication of these control signals. During each VPP dispatch cycle, the control center would transmit the charging/discharging data packet to each EV repeatedly until the control signal is successfully received and confirmed by this EV. On the other hand, it has been demonstrated in [24],[30] that communication delays of EV control signals are generally shorter than 100 milliseconds when the number of EVs is approximately one hundred, and are less than 2 seconds in the case of hundreds of EVs. For the VPP dispatch problem in this work, the communication duration T_c (30 seconds) is long enough with respect to the small sizes and time delays of these control signals, and thus the communication unreliability constraint will only affect the data acquisition and monitoring from RESs and EVs [31]. Therefore, it is an important and challenging work to analyze and model the impacts of imperfect communication on the data collection and information monitoring of RESs and EVs, and it becomes a significant task to propose an optimal and efficient scheme for the real-time VPP dispatch under various packet loss conditions.

C. Impacts of Imperfect Communications on RESs

The packet loss probability caused by imperfect communication will affect the renewable energy forecasting and V2G dispatch performance [27]. For the short-term forecasting of renewable generations, real-time monitoring information of WPPs and PVs should be combined with historical data [32]. Due to the intermittent availability of primary CR channels and the limited communication duration, monitoring information including solar irradiation, temperature, and wind speed transmitted from PVs and WPPs to the control center will be partially lost. Therefore, the decrease in the collected monitoring information would give rise to the drop in the accuracy of renewable energy forecasting. Based on the estimation model in [31], the predicted power outputs of WPPs and PVs, $\tilde{g}_t^{\mathrm{WPP}}$ and $\tilde{g}_t^{\mathrm{PV}}$, under the unreliable communication can be expressed as,

$$\tilde{g}_t^{\mathrm{WPP}} = \zeta_t^{\mathrm{WPP}} \cdot g_t^{\mathrm{WPP}} + (1-\zeta_t^{\mathrm{WPP}}) \cdot z_t^{\mathrm{WPP}} \quad (1)$$

$$\tilde{g}_t^{\mathrm{PV}} = \zeta_t^{\mathrm{PV}} \cdot g_t^{\mathrm{PV}} + (1-\zeta_t^{\mathrm{PV}}) \cdot z_t^{\mathrm{PV}} \quad (2)$$

$$\zeta_t^{\mathrm{WPP}} = \alpha_1 \cdot \zeta_0^{\mathrm{WPP}} + (1-\alpha_1) \cdot [\alpha_2 \cdot (1-\mu_t) + (1-\alpha_2) \cdot (L_t^{\mathrm{v}}/L)] \quad (3)$$

$$\zeta_t^{\mathrm{PV}} = \alpha_3 \cdot \zeta_0^{\mathrm{PV}} + (1-\alpha_3) \cdot [\alpha_4 \cdot (1-\mu_t) + (1-\alpha_4) \cdot (L_t^{\mathrm{v}}/L)] \quad (4)$$

where μ_t is the average packet loss probability of data communication at the tth time period; g_t^{WPP} and g_t^{PV} are the actual energy outputs of WPPs and PVs at time t; ζ_t^{WPP} and ζ_t^{PV} are the forecasting accuracy ratios of g_t^{WPP} and g_t^{PV}, respectively. As more monitoring data are transmitted successfully, the forecasting accuracy of RESs would be enhanced, and thus both of ζ_t^{WPP} and ζ_t^{PV} in (3) and (4) are decreasing functions with respect to the packet loss probability of transmitted monitoring data from RESs; ζ_0^{WPP} and ζ_0^{PV} are the initial forecasting accuracy ratios of g_t^{WPP} and g_t^{PV}, and their values can be determined by historical forecasting data; z_t^{WPP} and z_t^{PV} indicate the deviations between the predicted power outputs of RESs and the actual ones, and these two variables follow Gaussian distributions $z_t^{\mathrm{WPP}} \sim N(0, \sigma_1^2)$ and $z_t^{\mathrm{PV}} \sim N(0, \sigma_2^2)$, respectively [22]; L_t^{v} and L are the number of available communication channels at time t and total licensed channels in the CR network, respectively.

The short-term RES forecasting is performed every 15 minutes with rolling horizon procedures, and the forecasting accuracy is mainly affected by historical RES data and the real-time monitoring information transmitted under imperfect communication conditions [31]. In the estimation model (1)-(4), α_1, α_2, α_3, and α_4 are weight factors, and $0 < \alpha_1, \alpha_2, \alpha_3, \alpha_4 < 1$. Specifically, α_1 and α_3 are the weight factors of initial RES forecasting accuracy ratios determined by historical WPP and PV output data respectively. On the other hand, the short-term RES forecasting accuracy is firstly determined with an initial accuracy ratio, and would be improved based on the received real-time RES monitoring data. Then, the real-time monitoring data are influenced by the data packet loss probability and available communication channels in the CR network. Consequently, α_2 and α_4 are the weight factors to express the degree of impacts of the data packet loss probability and available CR channels on RES forecasting accuracies of WPPs and PVs.

Formulations (3)-(4) are typical multivariate linear regression models, and the values of weight factors α_1-α_4 can be solved and determined using the classical multiple linear regression analysis (MLRA) in [33] with historical RES and communication data in [7],[29],[32]. For larger values of α_1 and α_3, the real-time monitoring data would have less impact on the forecasting accuracy of RES power outputs, while larger values of α_2 and α_4 indicate the higher influence of data packet loss probability on the RES forecasting accuracy as well as the real-time VPP dispatch performance. Comparative studies and numerical results based on the MLRA show that factors α_1 and α_3 are usually in the range of 0.7-0.85 and factors α_2 and α_4 are between 0.4 and 0.6 under different RES output data and communication reliability conditions. In this case study, α_1, α_2, α_3, and α_4 are set to 0.8, 0.5, 0.8, 0.5 after a large number of simulation studies [29]. Besides, it is worth noting that, new monitoring data of WPP and PV outputs can be stored as the historical data, and the values of weight factors shall be recalculated and retuned regularly by combining the historical data with the updated real-time monitoring data on a daily basis.

In each dispatch cycle, the real-time monitoring data of RESs will be updated and transmitted to VPP control center for further analysis and optimization. In this study, when the real-time data on the power outputs of WPPs and PVs at current time t_0 are lost and unavailable, the RES power outputs at time t_0 are regarded to be the same as the values at the last cycle time t_0-1.

D. Impacts of Imperfect Communications on EVs

Communication reliability would also affect the estimation and prediction of EV parking behaviors. Compared with RESs, EV parking behaviors are much more difficult to forecast [34]. In this study, the parking model parameters of EVs, including the initial SOC distribution and the number of parking vehicles at any given point in time, follow Gaussian distributions as in [12]. Thus, multiple stochastic scenarios in the future horizons can be obtained from the historical data and Monte Carlo simulations [35] in order to capture the forecasting uncertainties, and each scenario expresses a possible operational status of EV parking behaviors with SOC values in each future dispatch time.

For the real-time operation, the smart meters implanted in EV chargers will send data packets at the current time, regarding the real-time SOC, EV arrival and departure time to the VPP control center. Nevertheless, the packet loss may occur due to the time

constraints of meter data communication [31]. When the data packets are unavailable, lacking the SOC and departure information of EVs, the VPP scheduling performance would be degraded [19]. Based on the estimation model of EV parking behaviors in [34], the EV arrival and departure behaviors under the unreliable communication can be formulated as follows,

$$\tilde{I}_{i,t}=\begin{cases}1 & u_{i,t}^{\text{out}}=1\ \&\ T_{\text{c0}}\le t\le T_i^{\text{out}},\quad \forall i\\ 1 & u_{i,t}^{\text{out}}=0\ \&\ T_{\text{c0}}\le t\le \tilde{T}_{i,s}^{\text{out}},\ \forall i,\ \forall s\\ 0 & \text{otherwise}\end{cases}\Bigg\}T_i^{\text{in}}\le T_{\text{c0}}$$
$$\Bigg\{\begin{matrix}1 & \tilde{T}_{i,s}^{\text{in}}\le t\le \tilde{T}_{i,s}^{\text{out}},\quad \forall i,\ \forall s\\ 0 & \text{otherwise}\end{matrix}\Bigg\}T_i^{\text{in}}>T_{\text{c0}} \tag{5}$$

$$u_{i,t}^{\text{out}}=\begin{cases}1 & \text{with probability of } 1-\mu_t\\ 0 & \text{with probability of } \mu_t\end{cases} \tag{6}$$

where $\tilde{I}_{i,t}$ is a binary variable to denote zero or one depending on whether the ith EV is stationary at the charging station or not at the tth time period; $u_{i,t}^{\text{out}}$ is also a binary variable depending on whether the departure time of the ith EV is collected or not under the packet loss probability of μ_t; $\tilde{T}_{i,s}^{\text{in}}$ and $\tilde{T}_{i,s}^{\text{out}}$ are the estimated arrival and departure time of the ith EV for scenario s, respectively. Here, in order to implement the rolling optimization considering the future horizons, the estimated arrival and departure time of the ith EV, $\tilde{T}_{i,s}^{\text{in}}$ and $\tilde{T}_{i,s}^{\text{out}}$, can be extracted from multiple stochastic scenarios, which is assumed to be the EV possible parking behaviors until its actual arrival and departure information is updated [36]. For the parking status of the ith EV, if its arrival time T_i^{in} is ahead of the beginning time of data communication duration T_{c0} in a dispatch cycle, the EV is available and schedulable for the VPP within this dispatch cycle. For the situation in which the EV fails to communicate its departure time T_i^{out}, its estimated departure time $\tilde{T}_{i,s}^{\text{out}}$ can be determined by the parking behavior of scenario s sampled from Gaussian distributions. Therefore, the estimated parking status of the schedulable EVs can be expressed in (5) and (6).

The EV chargers equipped with smart meters enable the VPP control center to dynamically estimate the number of schedulable EVs connected to the power grid. The real-time SOC information of EVs is required to calculate the available battery capacity for the VPP, while a part of the measurements cannot be acquired due to the lossy communication network [28]. In this study, when the real-time data on the SOC information of an EV are lost and unavailable, its SOC value at current time t_0 is assumed to be estimated by the SOC at time t_0-1 and the corresponding charging/discharging power.

E. Dynamic communication spectrum allocation

The CR is an emerging technique with the high flexibility to change its transmitter parameters based on the interaction with its environment [21]. The dynamic spectrum allocation (DSA) is utilized to provide CR networks with the capability to share the wireless spectrums among unlicensed users in an opportunistic manner, and thus can effectively overcome the spectrum inefficiency problems caused by the increased radio frequency demand [25]. There are two key actors in the DSA: 1) PU is the owner of a licensed channel and has the priority to use the spectrum; 2) SU is the opportunistic user which is allowed to sense the licensed spectrum and identify locally available channels in the absence of PU based on the temporal spectrum overlay [37]. In this paper, the scattered EVs and RESs act as SUs to dynamically access the CR channel, and the heterogeneous CR bandwidth from the PUs in the VPP can be offered for mobile EV users.

In order to alleviate the impacts of imperfect data communication, a DSA scheme is proposed considering the variable EV parking behaviors. Basically, the smart meters in EV chargers will participate in the spectrum allocation only when the EV is stationary at charging stations and connected to the power grid, and thus the number of SUs is time-varying in the DSA problem. In each dispatch cycle, the SUs shall be partitioned into L groups, and the SU in the lth group will always attempt to access the lth CR channel based on the *always-stay* scheme [37]. For each time slot in Fig. 2, a licensed channel can either be occupied by a PU or available for a SU, and smart meters can transmit the metering data to VPP through the allocated channels opportunistically. The data communication of a SU is successful only when the licensed channel is available and the SU wins the contention with other SUs in this group. Due to the probabilistic properties on the usage of channels by PUs and the competitions among SUs, the state of licensed channel l for the metering data packet communication can be modeled as an absorbing Markov chain process [25], and the state transition probability of a SU from the current time slot to the next time slot can be formulated as,

$$P_{m,m'}=\begin{cases}1-P_l^{\text{v}}+P_l^{\text{v}}\cdot(1-1/n_{l,t})+P_l^{\text{v}}\cdot 1/n_{l,t}\cdot P_{\text{e}}, & m'=m\\ P_l^{\text{v}}\cdot 1/n_{l,t}\cdot(1-P_{\text{e}}), & m'=m-1\\ 0, & \text{otherwise}\end{cases} \tag{7}$$

where $P_{m,m'}$ denotes the transition probability from the current state to the next state, in which there are m data packets to be transmitted in the current time slot and m' residual packets remaining in the next time slot; P_l^{v} is the probability of channel l to be available for SUs; $n_{l,t}$ is the number of SUs in group l at time t; P_{e} is the probability of packet communication error. For each time slot, when the channel l is free, a CR-driven SU in group l has a probability of $1/n_{l,t}$ to gain the permission of the channel [27]. Then, the state transition matrix $\mathbf{P}$ derived from the absorbing Markov chain for describing the data packet communication of a smart meter in a certain channel can be expressed as,

$$\mathbf{P}=\begin{bmatrix}P_{M,M} & \cdots & P_{M,m'} & \cdots & P_{M,0}\\ \vdots & \ddots & \vdots & \ddots & \vdots\\ P_{m,M} & \cdots & P_{m,m'} & \cdots & P_{m,0}\\ \vdots & \ddots & \vdots & \ddots & \vdots\\ P_{0,M} & \cdots & P_{0,m'} & \cdots & P_{0,0}\end{bmatrix} \tag{8}$$

where M is the number of total data packets to be transmitted by a SU. For a limited communication duration T_{c} with K time slots, the probability distribution vector over all transient states for a SU in group l at the tth time period can be obtained as follows,

$$\boldsymbol{\tau}_{l,t}^{K}=\boldsymbol{\tau}_{l,t}^{0}\cdot\Big(\prod_{k=1}^{K}\mathbf{P}\Big) \tag{9}$$

where $\prod_{k=1}^{K}\mathbf{P}$ denotes the multiplication of matrix $\mathbf{P}$ for K times; $\boldsymbol{\tau}_{l,t}^{K}$ is a row vector and its elements indicate the probabilities on the numbers of remaining data packets being [M, M-1, …, 1, 0] after the lapse of K time slots; $\boldsymbol{\tau}_{l,t}^{0}$ is the initial probability distribution and it shall be defined as $[1, 0, \ldots, 0, 0]$, in which nonezero elements correspond to the initial state $m=M$. The residual packets which fails to be transmitted during the limited duration T_{c} will be lost, and the average packet loss probability for a SU in group l at the tth time period can be calculated as follows,

$$\mu_{l,t} = \frac{1}{M}\sum_{m=0}^{M} m \cdot \boldsymbol{\tau}_{l,t}^{K}(m), \quad m \in [0,1,...,M] \tag{10}$$

where $\boldsymbol{\tau}_{l,t}^{K}(m)$ is an element of vector $\boldsymbol{\tau}_{l,t}^{K}$ to indicate the probability of m packets remaining at a SU after K time slots.

Hence, in order to minimize the average packet loss probability for all the groups of SUs at each dispatch period, a DSA model considering the variable behaviors of SUs can be formed to optimize the number of SUs in each channel group as,

$$\begin{aligned} \text{Min} \quad & \mu_t(n_{l,t}) = \frac{\sum_{l=1}^{L} \mu_{l,t} \cdot n_{l,t}}{N_{L,t}} \\ \text{s.t.} \quad & \sum_{l=1}^{L} n_{l,t} = N_{L,t} \end{aligned} \tag{11}$$

where $n_{l,t}$ is the positive integer variable to be optimized; $N_{L,t}$ is the total number of SUs at time t, and it can be determined as,

$$N_{L,t} = N_{\text{WPP}} + N_{\text{PV}} + \tilde{N}_{\text{EV},t} \tag{12}$$

$$\tilde{N}_{\text{EV},t} = \sum_{i=1}^{N_{\text{EV}}} \tilde{I}_{i,t} \tag{13}$$

where N_{WPP} and N_{PV} are the numbers of WPP and PV plants, respectively; $\tilde{N}_{\text{EV},t}$ varies with different dispatch cycle time and equals to the total number of EVs connected to the power grid at charging stations; N_{EV} is the total number of EVs in the VPP. The DSA model is a typical integer linear program problem and can be performed with the freely available YALMIP toolbox [38] in MATLAB platform and readily solved using the CPLEX solver.

III. Modelling and Methodology

The profit maximization problem of a VPP can be formulated as a classical two-stage mixed-integer stochastic programming to cope with the uncertainties in the VPP scheduling process [7]. The first stage is the day-ahead scheduling to solve here-and-now decisions which should be made before all the uncertainties become known, while wait-and-see decisions are used as countermeasures in the real-time scheduling for the energy mismatch between the day-ahead forecasting and actual realization [35].

A. Day-Ahead Scheduling

The day-ahead scheduling implements a stochastic bidding strategy with here-and-now decisions to determine the optimal amount of sold/purchased electricity over a 24-hour horizon in order to maximize the expected economic revenue [5], while the uncertainties in WPP and PV outputs, day-ahead and balancing market prices, EV parking behaviors are considered and represented by various stochastic scenarios based on the historical data in [7],[34],[36]. Hence, the day-ahead objective function for the expected profit maximization consists of the amounts of electricity sold/purchased in the day-ahead market $G_{t,s}^{\text{a}}$, downward electricity sold in the balancing market $G_{t,s}^{\text{down}}$, and upward electricity purchased in the balancing market $G_{t,s}^{\text{up}}$, as well as the battery degradation cost and charging revenue of EVs under scenario s, as follows,

$$\begin{aligned} \text{Max} \ \sum_{t=1}^{N_{\text{T}}}\sum_{s=1}^{N_s} \pi_s \cdot [\lambda_{t,s}^{\text{a}} \cdot (G_{t,s}^{\text{a}} + G_{t,s}^{\text{down}} \cdot \delta_{t,s}^{\text{down}} - G_{t,s}^{\text{up}} \cdot \delta_{t,s}^{\text{up}}) \\ + \sum_{i=1}^{N_{\text{EV}}} (F_{i,t,s}^{\text{EV}} - C_{i,t,s}^{\text{EV}})] \end{aligned} \tag{14}$$

where N_{T} is the total number of time periods in the day-ahead scheduling horizon; N_s is the number of scenarios for stochastic optimization; π_s is the probability of scenario s, and the sum of probabilities for all scenarios is equal to 1; $\lambda_{t,s}^{\text{a}}$ is the electricity price in the day-ahead market at time t under scenario s; $\delta_{t,s}^{\text{down}}$ and $\delta_{t,s}^{\text{up}}$ are downward and upward balancing price ratios, respectively. In the balancing market, the VPP can only purchase the balancing energy with a higher upward balancing price than the day-ahead power price, and sell electricity at a lower downward balancing price [29]. Here, due to the uncertainties in the balancing market prices, the downward and upward balancing prices are also uncertain and can be represented by stochastic scenarios with associated occurrence probabilities in the proposed VPP model [40]. Also, $F_{i,t,s}^{\text{EV}}$ is the total charging revenue of the ith EV leaving at time t, as follows,

$$F_{i,t,s}^{\text{EV}} = \lambda_{\text{ch}} \cdot (SOC_{i,T_i^{\text{out}},s} - SOC_{i,T_i^{\text{in}},s}) \cdot E_i, \ \forall i, \ \forall t, \ \forall s \tag{15}$$

where $SOC_{i,T_i^{\text{in}},s}$ and $SOC_{i,T_i^{\text{out}},s}$ are the initial arrival and final departure SOC values of the ith EV under scenario s, respectively; λ_{ch} is the EV charging price in the VPP, and it is usually lower than the market price [6]. Here, λ_{ch} is set to 35\$/MWh.

The most popular lithium-ion battery, as used in Tesla Model S and Honda Fit EVs, is adopted to evaluate the battery degradation cost $C_{i,t,s}^{\text{EV}}$ caused by the charging/discharging of EVs [9],

$$C_{i,t,s}^{\text{EV}} = \frac{d_i C_i^{\text{c}} [(1+d_i)^{\frac{0.2E_i}{c_i E_i^{\text{m}}}} - 0.6]}{E_i^{\text{m}} [(1+d_i)^{\frac{0.2E_i}{c_i E_i^{\text{m}}}} - 0.6]} \cdot (\eta_i^{\text{ch}} g_{i,t,s}^{\text{ch}} + \frac{g_{i,t,s}^{\text{dis}}}{\eta_i^{\text{dis}}}), \forall i, \forall t, \forall s \tag{16}$$

where C_i^{c} is the EV's battery capital cost including replacement costs; $g_{i,t,s}^{\text{ch}}$ and $g_{i,t,s}^{\text{dis}}$ denote the charging and discharging energy of the ith EV during the tth time period under scenario s; η_i^{ch} and η_i^{dis} are the charging and discharging efficiencies of EV batteries; E_i and E_i^{m} are the battery capacity and the mean daily amount of processed energy of the ith EV, respectively; d_i and c_i are the equivalent daily discount rate and wear coefficient, respectively.

In the optimal scheduling model, the SOC of each EV battery should be limited to avoid the overcharging and overdischarging, and also shall be charged with the required amount of energy before its leaving time T_i^{out} [41], as follows,

$$SOC_{i,\min} \le SOC_{i,t,s} \le SOC_{i,\max}, \quad \forall i, \forall t, \forall s \tag{17}$$

$$SOC_{i,T_i^{\text{out}},s} \ge SOC_i^{\text{out}} \quad \forall i, \ \forall s \tag{18}$$

$$SOC_{i,t,s} = SOC_{i,t\text{-}1,s} + (\eta_i^{\text{ch}} \cdot g_{i,t,s}^{\text{ch}} - \frac{1}{\eta_i^{\text{dis}}} \cdot g_{i,t,s}^{\text{dis}}) \cdot \frac{1}{E_i}, \ \forall i, \forall t, \forall s \tag{19}$$

$$SOC_{i,T_i^{\text{out}},s} = SOC_{i,T_i^{\text{in}},s} + \sum_{t=1}^{T_i^{\text{out}}-1} (\eta_i^{\text{ch}} \cdot g_{i,t,s}^{\text{ch}} - \frac{1}{\eta_i^{\text{dis}}} \cdot g_{i,t,s}^{\text{dis}}) \cdot \frac{1}{E_i}, \ \forall i, \forall s \tag{20}$$

where $SOC_{i,\min}$ and $SOC_{i,\max}$ are the lower and upper bounds of SOC of the ith EV; $SOC_{i,t,s}$ and SOC_i^{out} are the SOC of the ith EV at time t and its required SOC at the departure time, respectively. As the fast charging/discharging rate will degrade the performance of EV batteries and shorten the lifespan [10], the charging/discharging energy of EVs shall be limited as,

$$0 \le g_{i,t,s}^{\text{ch}} \le g_{i,\max}^{\text{ch}} \cdot u_{i,t,s} \cdot I_{i,t,s}, \ \forall i, \forall t, \forall s \tag{21}$$

$$0 \le g_{i,t,s}^{\text{dis}} \le g_{i,\max}^{\text{dis}} \cdot v_{i,t,s} \cdot I_{i,t,s}, \ \forall i, \forall t, \forall s \tag{22}$$

$$u_{i,t,s} + v_{i,t,s} \le 1, \ \forall i, \forall t, \forall s \tag{23}$$

where $g_{i,\max}^{\text{ch}}$ and $g_{i,\max}^{\text{dis}}$ are the allowable maximum charging and discharging energy, respectively; $u_{i,t,s}$ and $v_{i,t,s}$ are binary variables denoting the state of EV battery energy flow, charging or discharging, at time t; $I_{i,t,s}$ is also a binary variable to denote 0 or 1 depending on whether the ith EV is available at time t.

Constraints (21)-(23) ensure that each EV can only schedulable when the EV is connected to the grid, and the battery charging and discharging cannot be performed simultaneously.

For each scheduling period under each scenario, the energy balance equality constraints between the energy production and consumption in the VPP should be considered as follows,

$$g_{t,s}^{\mathrm{WPP}} + g_{t,s}^{\mathrm{PV}} + G_{t,s}^{\mathrm{up}} + \sum_{i=1}^{N_{\mathrm{EV}}} g_{i,t,s}^{\mathrm{dis}} = G_{t,s}^{\mathrm{a}} + G_{t,s}^{\mathrm{down}} + \sum_{i=1}^{N_{\mathrm{EV}}} g_{i,t,s}^{\mathrm{ch}}, \forall t, \forall s \quad (24)$$

$$G_t^{\mathrm{a}} = G_{t,1}^{\mathrm{a}} = G_{t,2}^{\mathrm{a}} = \cdots = G_{t,Ns}^{\mathrm{a}}, \quad \forall t \quad (25)$$

where G_t^{a} denotes the optimal amount of sold/purchased electricity submitted to the day-ahead market at the tth time period. Constraint (25) ensures that the VPP can only submit one bidding curve at each time period for all the scenarios [7].

B. Interactive Optimization of VPP Dispatch and DSA

Based on the optimal bidding results in the day-ahead market, the real-time dispatch stage with wait-and-see decisions schedules the charging/discharging of EVs and the transactions with the balancing market to settle the deviations between the contracted and actual energy outputs of the VPP [39],[42]. In general, the day-ahead scheduling is implemented on an hourly basis, while the real-time operation updates the dispatch of VPP resources with a more frequent time interval (e.g., 15 minutes). Here, a scenario-based real-time VPP dispatch with RHO strategy in [6] is implemented. Due to the volatility of RES outputs and time-varying EV parking behaviors, the failed and late delivery of real-time monitoring information on EVs and RESs would result in the degradation of VPP dispatch performance, and hence an optimal DSA scheme considering the variable SUs in each possible scenario in the future horizons is obligatory to enhance the reliability and availability of CR communication networks. Consequently, an interactive approach is proposed to dynamically optimize the CR spectrum allocation and EV dispatch for improving VPP benefits under imperfect communication effects.

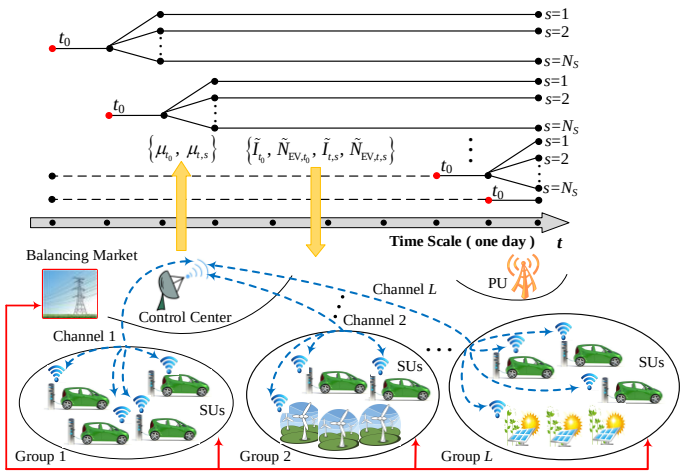

Fig. 3 Scenario-based interactive framework of VPP dispatch and DSA

Fig. 3 schematically depicts the proposed interactive framework for the combined optimization of VPP dispatch and DSA scheme. In the RHO based VPP dispatch, each rolling decision step solves for the current dispatch cycle and looks ahead the remaining dispatch cycles considering the uncertainties of real-time power price, WPP and PV outputs as well as EV parking behaviors in future horizons. It is worth to note that the variable number of schedulable EVs in the VPP dispatch model determines the number of SUs in the optimization model of DSA in (11)-(13), and the CR spectrums can be pre-allocated based on the estimated EV parking behaviors for all the future scenarios. On the other hand, the packet loss probability of CR networks determined by the DSA will affect the real-time monitoring and scheduling performance for EVs. Thus, the lowest packet loss probability will be resulted with the improved communication network for each dispatch cycle, and EV charging/discharging actions can be rescheduled continuously based on the updated real-time information (e.g., EV arrivals and their battery SOC) to further decrease the VPP operation cost.

In the scenario-based stochastic RHO strategy, the optimization objective is to minimize the total operation cost, including the real-time transactional cost for balancing electricity and the battery degradation cost of EVs at the current time t_0, plus the expected operation cost of all the future scenarios, as follows,

$$\begin{aligned} \mathrm{Min} \quad & (G_{t_0}^{\mathrm{r}} \cdot \lambda_{t_0}^{\mathrm{r}}) + \sum_{i=1}^{N_{\mathrm{EV}}} \tilde{I}_{i,t_0} \cdot C_{i,t_0}^{\mathrm{EV}} \\ & + \sum_{s=1}^{N_s} \pi_s \cdot \sum_{t=t_0+1}^{N_{\mathrm{T}}} [(G_{t,s}^{\mathrm{r}} \cdot \lambda_{t,s}^{\mathrm{r}}) + \sum_{i=1}^{N_{\mathrm{EV}}} \tilde{I}_{i,t,s} \cdot C_{i,t,s}^{\mathrm{EV}}] \end{aligned} \quad (26)$$

where $\lambda_{t_0}^{\mathrm{r}}$ and $\lambda_{t,s}^{\mathrm{r}}$ are the real-time power prices in the balancing market at the current time t_0 and time t under scenario s, respectively; $G_{t_0}^{\mathrm{r}}$ and $G_{t,s}^{\mathrm{r}}$ are the amounts of electricity purchased/sold in the balancing market at time t_0 and time t under scenario s, respectively; $\tilde{I}_{i,t_0}$ and $\tilde{I}_{i,t,s}$ are the parking status of the ith EV at time t_0 and time t under scenario s; C_{i,t_0}^{EV} and $C_{i,t,s}^{\mathrm{EV}}$ are the battery degradation cost of the ith EV at time t_0 and time t under scenario s, and their values can be calculated from (16).

The operational constraints (17)-(25) in the day-ahead scheduling can also be used in the real-time dispatch model. It should be pointed out that the amount of sold/purchased electricity in the day-ahead market G_t^{a} for each time period shall be a constant in the real-time operation stage [7]. Moreover, the energy balance equality constraints at the current time t_0 and the remaining time periods under scenario s should be considered and expressed as,

$$g_{t_0}^{\mathrm{WPP}} + g_{t_0}^{\mathrm{PV}} + G_{t_0}^{\mathrm{r}} + \sum_{i=1}^{N_{\mathrm{EV}}} \tilde{I}_{i,t_0} \cdot g_{i,t_0}^{\mathrm{dis}} = G_{t_0}^{\mathrm{a}} + \sum_{i=1}^{N_{\mathrm{EV}}} \tilde{I}_{i,t_0} \cdot g_{i,t_0}^{\mathrm{ch}} \quad (27)$$

$$\tilde{g}_{t,s}^{\mathrm{WPP}} + \tilde{g}_{t,s}^{\mathrm{PV}} + G_{t,s}^{\mathrm{r}} + \sum_{i=1}^{N_{\mathrm{EV}}} \tilde{I}_{i,t,s} \cdot \tilde{g}_{i,t,s}^{\mathrm{dis}} = G_t^{\mathrm{a}} + \sum_{i=1}^{N_{\mathrm{EV}}} \tilde{I}_{i,t,s} \cdot \tilde{g}_{i,t,s}^{\mathrm{ch}} \quad (28)$$

$$t \in [t_0+1, N_{\mathrm{T}}], \forall s$$

where $\tilde{g}_{i,t,s}^{\mathrm{ch}}$ and $\tilde{g}_{i,t,s}^{\mathrm{dis}}$ denote the charging and discharging energy of the ith EV at time period t under scenario s, respectively. Here, a positive value of G_t^{a} signifies that the electricity is sold to the day-ahead market, while a positive value of $G_{t,s}^{\mathrm{r}}$ represents the electricity purchased from the balancing market. Also, $g_{i,t,s}^{\mathrm{ch}}$, $g_{i,t,s}^{\mathrm{dis}}$, $\tilde{g}_{i,t,s}^{\mathrm{ch}}$, $\tilde{g}_{i,t,s}^{\mathrm{dis}}$, $G_{t_0}^{\mathrm{r}}$, and $G_{t,s}^{\mathrm{r}}$ are the decision variables to be optimized in the real-time RHO strategy.

In summary, the execution flowchart of the proposed coordinated EV scheduling with DSA scheme is illustrated in Fig. 4. It is worth noting that, with the optimized CR network, the set of possible scenarios from time periods t_0+1 to N_{T} shall be updated in each dispatch cycle based on new real-time communication data on the EV arrival/departure information, and the VPP only implements the obtained decision for the current time t_0. This scenario-based RHO procedure will be repeated iteratively until the end of scheduling horizons.

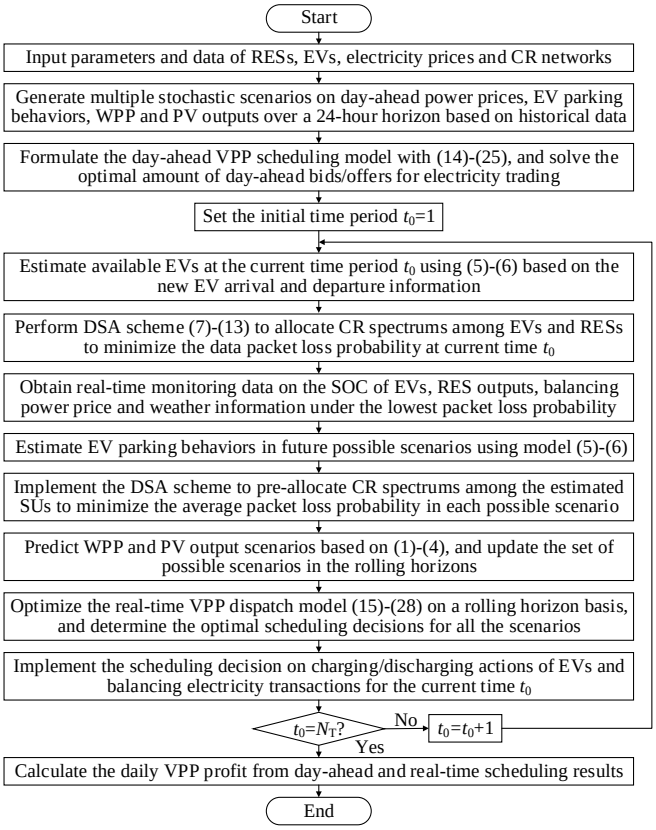

Fig. 4 Flowchart of interactive optimization of VPP dispatch and DSA scheme

IV. Case Study

A. System Data

The studied VPP consists of 2000 EVs with different battery capacities, a WPP with a total capacity of 10MW, and a PV plant with a total capacity of 9MW. Five types of EVs, including BMW i3, Venturi Fetish, Nissan Leaf, Tesla Model S, and Honda Fit in [35],[43], are selected as representative EVs with equal parking probabilities at charging stations. The electrical characteristics of EV batteries are adopted from [9],[43], as listed in Table I, and the statistical data on EVs' arrival/departure time and initial SOC are gathered from [35],[36],[44]. The actual energy outputs of the WPP and PV are extracted from historical data in [45],[46]. The power price data in day-ahead and balancing markets from [7],[47] are used to generate possible scenarios for day-ahead and real-time scheduling. In the day-ahead scheduling, the scenario-based model is used to represent the uncertainties in electricity prices, EV behaviors, WPP and PV outputs with the initial stochastic scenarios of 10000, and the scenario reduction is utilized to decrease the number of scenarios into 100 so as to lower the scale and computation time of this stochastic model [35],[40].

In the real-time RHO strategy, various stochastic scenarios of WPP and PV outputs can be obtained based on (1)-(4) to capture RES forecasting uncertainties under a given packet loss probability, where the parameters are set as $\sigma_1=\sigma_2=1$ and $\zeta_0^{\mathrm{WPP}}=\zeta_0^{\mathrm{PV}}=0.6$ [30],[32]. Hence, the scenario trees can be formed with a set of operational scenarios in which each scenario expresses a possible status with electricity prices, RES outputs and EV parking behaviors in the remaining time periods. The initial scenario tree of the real-time dispatch has 2000 scenarios, with a possibility of 1/2000 for each scenario. Then, a scenario reduction technique in [48] is used to decrease the number of initial scenarios into 10 while retaining a good approximation of system uncertainties.

TABLE I
Electrical Characteristics of Selected EV Batteries [9],[43]

EV Model	Battery capacity (kWh)	Maximum charging/discharging power (kW)	Charging/discharging efficiency (%)	Battery capital cost ($/kWh)
BMW i3	22	4.6	93	168
Venturi Fetish	54	9.8	92	150
Nissan Leaf	24	6.9	93	163
Tesla Model S	85	10.0	90	244
Honda Fit	20	6.6	90	122

The stochastic day-ahead scheduling and the RHO-based real-time dispatch models in (14)-(28) are both mixed-integer linear programming problems which can be modeled by YALMIP and solved by CPLEX Optimizer [38] on a personal computer with 4-GHz Intel Core i7 CPU and 64GB RAM. In the DSA model in (7)-(13), the number of licensed CR channels are set to 30 [22], and the available probabilities of these channels for SUs follow a uniform distribution $P_l^{\mathrm{v}} \sim U(0.2, 0.8)$ with $P_{\mathrm{e}} = 0.1$ [27]. In each dispatch cycle, the data communication duration T_{c} is 30 seconds, and the length of each time slot is 200 milliseconds. Also, the number of data packets to be transmitted by each SU is $M = 5$ [27].

B. Comparative Results and Analysis

In this study, four comparative schemes are considered for in-depth investigations on the effectiveness and superiority of the proposed methodology: 1) Scheme 1 is the proposed interactive approach in Sections III; 2) Scheme 2 performs the DSA scheme from [27] in which the time-varying number of SUs is not considered; 3) Scheme 3 adopts the pervasive distributed spectrum access in [49] for WiFi or wireless local area network where SUs can dynamically access available spectrums based on their traffic demands without the centralized DSA execution; 4) Scheme 4 implements the two-stage VPP scheduling without considering the battery degradation cost in (16). The amounts of day-ahead VPP electricity trading with various price scenarios are shown in Fig. 5. It can be found that, a large amount of electricity is sold to the day-ahead market in hours 9-13 due to high power prices during these periods. Since the battery degradation cost of EVs is not considered in Scheme 4, the day-ahead VPP electricity trading in this scheme is more frequent than other three schemes.

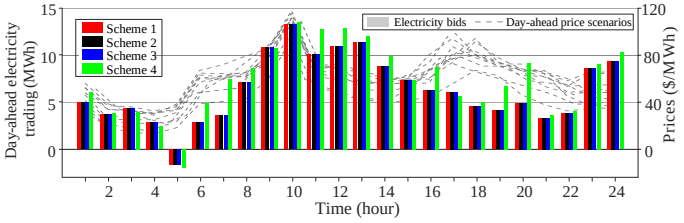

Fig. 5. Day-ahead electricity bids of the VPP with schemes 1-4

In the real-time dispatch stage, Fig. 6 depicts the number of available EVs at charging stations for different time periods. Fig. 7-9 provide the comparative performances on the average packet loss probability, the charging/discharging energy of EVs, and the electricity sold/purchased in the balancing market with schemes 1-4 over a 24-hour horizon. The charging/discharging power outputs of different types of EVs with the proposed scheme is further illustrated in Fig. 10. The statistical data of VPP scheduling results are listed in Table II. Highlights from the results are summarized as follows: 1) As the time-varying number of EVs participating in the DSA is considered based on RHO strategy in scheme 1, the packet loss probability in this scheme is the lowest compared to the fixed spectrum allocation in scheme 2 and the distributed spectrum selection in scheme 3, and hence the proposed scheme 1 can remarkably outperform other schemes on

the real-time VPP operation cost and daily profit; 2) In Fig. 8-9 and Table II, the amounts of EV charging/discharging energy as well as day-ahead and real-time electricity trading in scheme 4 are much larger than those of schemes 1-3. As a result, the day-ahead VPP revenue from the day-ahead market is the highest in this scheme due to the frequent charging/discharging of EVs, while the lower VPP profit with higher operation cost is resulted.

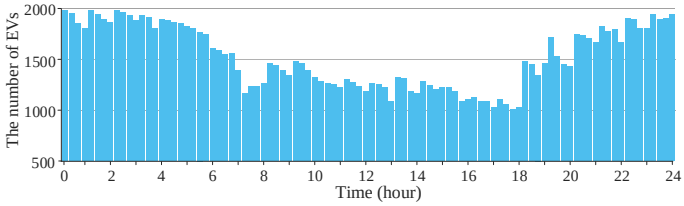

Fig. 6. Real-time number of EVs stationary at charging stations

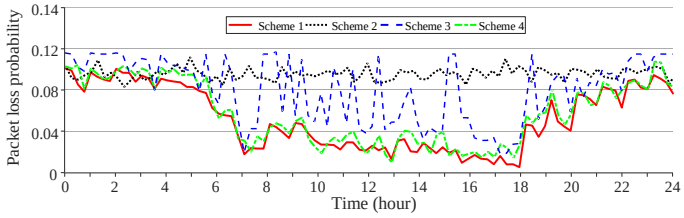

Fig. 7. Average packet loss probability with schemes 1-4

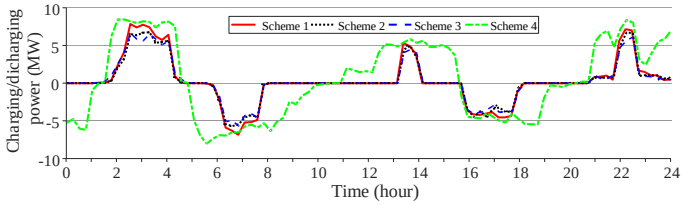

Fig. 8. Real-time charging/discharging power of EVs with schemes 1-4

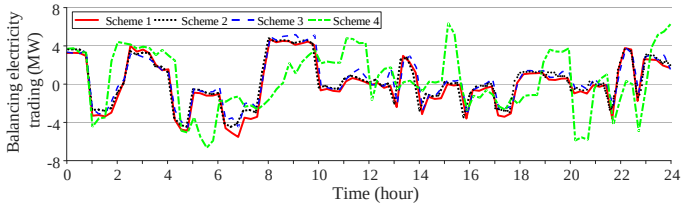

Fig. 9. Real-time electricity trading in the balancing market with schemes 1-4

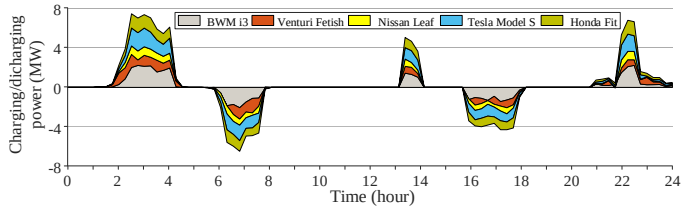

Fig. 10. Charging/discharging power outputs of five types of EVs with scheme 1

TABLE II
COMPARATIVE ECONOMIC PERFORMANCE RESULTS OF SCHEMES 1-4

Scheme	1	2	3	4
Day-ahead revenue ($)	8729.73	8729.73	8729.73	**8931.36**
Balancing electricity purchased (MWh)	55.35	60.75	56.41	70.55
Balancing electricity sold (MWh)	31.18	28.71	25.69	41.39
Balancing transaction cost ($)	176.08	533.79	671.70	**683.17**
Battery degradation cost ($)	749.70	720.03	**683.17**	1674.80
Real-time operation cost ($)	**925.78**	1253.82	1354.87	1841.88
Total daily VPP profit ($)	**8121.24**	7786.52	7706.22	7440.22

Fig. 11-14 illustrate the comparative scheduling performances with the increase of the number of EVs from 1000 to 3000. It can be found that, with the increased number of EVs, the data packet loss probability remarkably increases, while the real-time operation cost and EV battery degradation cost also gradually rise. The results can further confirm the superior performance of the proposed scheme 1, especially on the real-time operation cost and daily VPP profit. It is noted that, compared with schemes 2 and 3, scheme 1 exhibits higher EV battery degradation cost with larger amount of EV charging/discharging power to decrease the real-time transactional cost in the balancing market. Moreover, although the packet loss probability increases with the rising number of EVs, the total daily profit of VPP can gradually be raised due to the increased battery storage capacity.

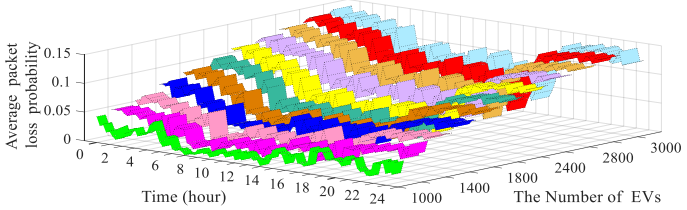

Fig. 11. Packet loss probability versus different numbers of EVs with scheme 1

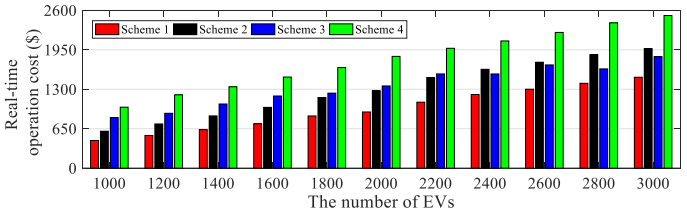

Fig. 12. Real-time operation cost versus different numbers of EVs

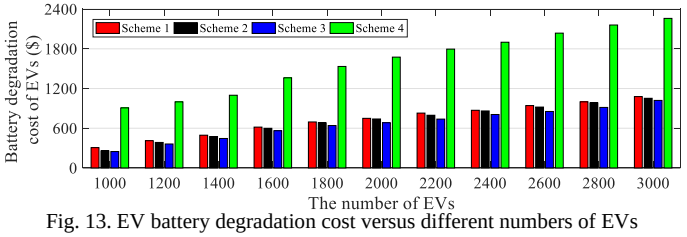

Fig. 13. EV battery degradation cost versus different numbers of EVs

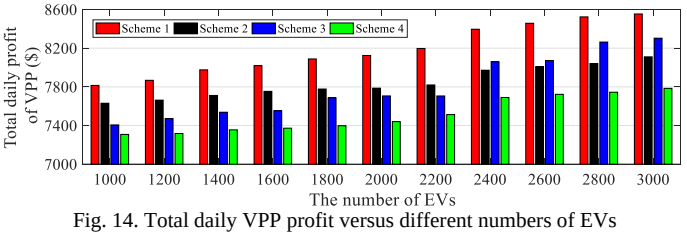

Fig. 14. Total daily VPP profit versus different numbers of EVs

C. *Effects of Communication Conditions on VPP Performances*

In order to investigate the effect of different communication conditions on VPP scheduling performances with the proposed scheme, Fig. 15 shows the results of real-time operation cost, EV battery degradation cost and daily profit under different packet loss probability varying from 0 to 0.9 with the parameter settings in Section IV.A. With the increased packet loss probability, the operation cost increases while the daily VPP profit rapidly decreases. It can also be found that, as the less number of EVs is detected under the higher packet loss probability, the battery degradation cost tends to be slightly reduced. Furthermore, Fig. 16-17 illustrate the effects of the number of licensed channels in the CR network and the available probability of CR channels from PUs on the daily VPP profit, respectively. The comparative results demonstrate that the proposed scheme can effectively coordinate and optimize the CR channels and V2G dispatch in an interactive way to enhance the monitoring and control performance of EVs under various imperfect communication conditions.

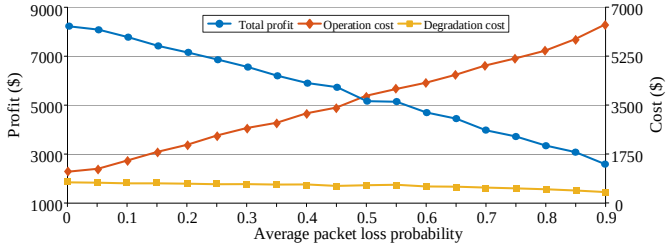

Fig. 15. Effects of packet loss probability on VPP scheduling performances

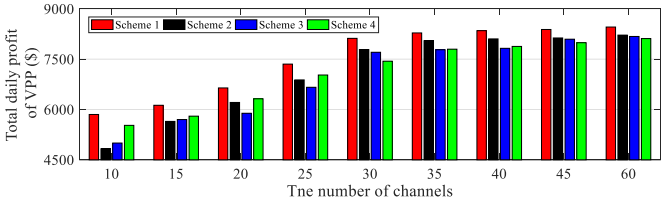

Fig. 16. Effects of different numbers of licensed channels on daily VPP profit

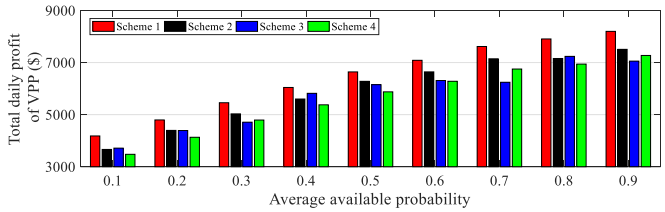

Fig. 17. Effects of average available probability of PUs on daily VPP profit

D. Discussion

For the wait-and-see decision making process in the real-time VPP dispatch, multiple possible scenarios in the future horizons are derived from the basis values of short-term forecasting results, and Monte Carlo simulations are implemented to form a set of scenarios by sampling from Gaussian probability distributions of short-term forecasting errors on RES outputs, power prices and EV parking behaviors. Taking the WPP output as an example, Fig. 18 shows the simulation results of scenario generation and reduction in the real-time dispatch stage. It can be found from Fig. 18 (a) that, due to the small real-time forecasting errors, the initial stochastic scenarios distribute densely around short-term forecasting values within a narrow range. Then, the scenario reduction method is used to remove the scenarios with many similarities to others while retaining the essential properties of the initial scenarios [48], as depicted in Fig. 18 (b).

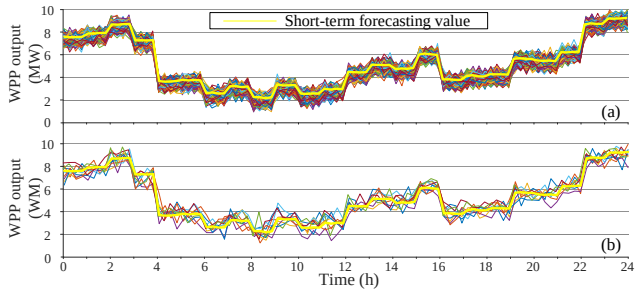

Fig. 18. Scenario generation and reduction results of WPP outputs in the real-time dispatch stage: (a) Initial scenarios; (b) Reduced scenarios

TABLE III
TOTAL DAILY VPP PROFITS UNDER DIFFERENT NUMBERS OF SCENARIOS ($)

# of initial scenarios	# of scenarios after scenario reduction					
	5	10	20	30	50	100
500	7906.53	7948.79	7959.61	7988.46	8013.10	8033.66
1000	7928.82	8020.34	8040.67	8090.30	8093.39	8134.04
2000	8027.43	**8121.24**	8161.87	8173.67	8211.93	8251.29
4000	8035.62	8137.19	8170.68	8178.99	8220.48	8265.04
6000	8042.96	8139.52	8174.07	8183.93	8229.50	8270.48
8000	8047.28	8145.44	8179.47	8192.92	8237.84	8276.07
10000	8051.69	8149.24	8184.49	8199.26	8255.30	8287.08

TABLE IV
AVERAGE SIMULATION TIME UNDER DIFFERENT NUMBERS OF SCENARIOS (S)

# of initial scenarios	# of scenarios after scenario reduction					
	5	10	20	30	50	100
500	14.43	26.63	49.15	146.95	215.32	579.40
1000	15.06	27.09	49.93	147.02	216.84	580.02
2000	16.74	**28.85**	50.79	147.96	220.89	582.79
4000	18.28	30.07	51.64	149.07	221.29	584.63
6000	19.06	33.29	54.45	151.27	224.78	587.38
8000	22.68	35.64	56.27	154.89	227.67	590.49
10000	25.49	39.77	60.22	156.98	232.51	594.58

The comparative studies with different numbers of stochastic scenarios have further been performed to investigate the scalability and real-time applicability of the scenario-based RHO strategy. Tables III and IV show the results of daily VPP profit and average simulation time under various numbers of original and reduced scenarios. It can be found that, with the increased number of initial and reduced scenarios, the VPP profit would be slightly enhanced, while the computation time would dramatically rise. Under the same number of reduced scenarios, the tests with more than 2000 initial scenarios have approximate daily profit results. Also, with the number of reduced scenarios beyond 10, the computation time is usually over half a minute, which cannot be applicable to the real-time dispatch problem in this study. Compared with the day-ahead scheduling, the scenarios of RES outputs and EV behaviors in the real-time RHO dispatch are generated from the short-term forecasting and estimation models (1)-(6) and updated using the real-time monitoring data with higher resolutions based on rolling procedures, and therefore the less number of reduced scenarios can exhibit satisfactory dispatch performance and solution accuracy [35]. As a compromise between the total VPP profit and real-time applicability, the settings with 2000 initial scenarios and 10 reduced scenarios appear to be an appropriate trade-off choice to satisfy both the solution accuracy and computational efficiency. Furthermore, it should be pointed out that, the required computation time without the scenario reduction is generally over half an hour and absolutely cannot satisfy the real-time requirement of VPP dispatch problems [7].

Generally, distributed control methods are effective ways to actively lower the required amount of information transfer and exchange among numerous EVs, and thus less communication bandwidth would be required [50]. As these EVs will only send a small amount of global information and keep the private information internally, the problem of data packet loss can be avoided with the distributed method. However, since the number of EVs participating in the real-time VPP dispatch is time-varying and unknown in the future horizons due to the variable EV parking behaviors, multiple optimized agents in the distributed method would vary dramatically during the iterative solution procedures. As a result, the convergence of boundary exchanged variables will suffer sharp variations and oscillation issues in the distributed optimization process, leading to local optimal solutions or even the failures of convergence after a limited number of iterations.

In this study, the distributed method in [50] is introduced and compared with the proposed approach, and the VPP scheduling problem can be decomposed into 2000 local EV dispatch subproblems with reduced complexity. Each EV solves the optimization subproblem with the continuously updated Lagrangian multipliers to minimize its local operation cost, and determines the amount of charging/discharging electricity it is willing to offer. Simulation results show that the total daily profit and real-time operation cost of the distributed method are $ 7967.51 and

$ 991.92, while the proposed approach can achieve better performance on the total daily profit $ 8121.24 with lower operation cost $ 925.78. Consequently, it can be concluded that, though the distributed method can achieve EV decision autonomy with less communication bandwidth, this method is not applicable to solve the VPP scheduling problem with time-varying EV agents.

V. Conclusion

In this paper, an interactive approach is proposed for the joint dynamic optimization of CR spectrum allocation and VPP dispatch to coordinate charging/discharging strategies of massive and dispersed EVs. The following are the findings of this study: 1) The data packet loss in communication networks has been found to have a significant influence on the monitoring and controlling performance of EVs, and the proposed approach can effectively enhance the V2G communication reliability and the daily VPP profit; 2) With the increased number of EVs from 1000 to 3000, the packet loss probability in CR networks would rise, and thus the increasing EV battery degradation and real-time operation costs are resulted, while the VPP profit can be gradually enhanced due to the increased EV battery capacity; 3) The proposed approach has been fully evaluated under various imperfect communication effects, and comparative studies confirm its superior capability to solve the large-scale scattered EV dispatch problem with limited communication spectrum resource. Further on-going research would focus on the joint spatial and temporal spectrum sharing for CR enabled V2G dispatch problems, in which the impacts of distances between SUs and VPP control center on the communication reliability is considered.

References

[1] W. Su, H. Eichi, and W. Zeng, *et al.* "A survey on the electrification of transportation in a smart grid environment," *IEEE Trans. Ind. Informat.,* vol. 8, no. 1, pp. 1-10, Feb. 2012.

[2] D. Dallinger, J. Link, and M. Buttner, "Smart grid agent: Plug-in electric vehicle," *IEEE Trans. Sustain. Energy*, vol. 5, no. 3, pp. 710-717, Jul. 2014.

[3] International Energy Agency (2016). *Global EV Outlook Understanding the Electric Vehicle Landscape to 2020, Clean Energy Ministerial. Report 1,* accessed on Jul. 10, 2016. [Online]. Available: https://www.iea.org/publications/freepublications/publication/Global_EV_Outlook_2016.pdf

[4] W. Kempton and J. Tomić, "Vehicle-to-grid power fundamentals: Calculating capacity and net revenue," *J. Power Sources,* vol. 144, no. 1, pp. 268-279, Apr. 2005.

[5] Q. Zhao, Y. Shen, and M. Li, "Control and bidding strategy for virtual power plants with renewable generation and inelastic demand in electricity markets," *IEEE Trans. Sustain. Energy*, vol. 7, no. 2, pp. 1034-1042, Apr. 2016.

[6] M. Vasirani, R. Kota, and R. L. G. Cavalcante, *et al.* "An agent-based approach to virtual power plants of wind power generators and electric vehicles," *IEEE Trans. Smart Grid*, vol. 4, no. 3, pp. 1314-1322, May 2013.

[7] H. Pandžić, J. M. Morales and A. J. Conejo, *et al.* "Offering model for a virtual power plant based on stochastic programming," *Appl. Energy,* vol. 105, pp. 282–292, May 2013.

[8] R. Gough, C. Dickerson, and P. Rowley, *et al.* "Vehicle-to-grid feasibility: A techno-economic analysis of EV-based energy storage," *Appl. Energy,* vol. 192, pp. 12–23, Apr. 2017.

[9] H. Farzin, M. Fotuhi-Firuzabad, and M. Moeini-Aghtaie, "A practical scheme to involve degradation cost of lithium-ion batteries in vehicle-to-grid applications," *IEEE Trans. Sustain. Energy*, vol. 7, no. 4, pp. 1730-1738, Oct. 2016.

[10] G. Yan, D. Liu, and J. Li *et al*., "A cost accounting method of the Li-ion battery energy storage system for frequency regulation considering the effect of life degradation," *Protection Control Modern Power Syst*., pp. 43-51, Feb. 2018, DOI: 10.1186/s41601-018-0076-2.

[11] V2G Global Roadtrip: around the world in 50 projects. Accessed on Oct. 2018. [Online]. Available: http://everoze.com/app/uploads/2018/10/UKPN001-S-01-H-V2G-global-review-compressed.pdf.

[12] R. Yu, W. Zhong, and S. Xie, *et al.,* "Balancing power demand through EV mobility in vehicle-to-grid mobile energy networks," *IEEE Trans. Ind. Informat.*, vol. 12, no. 1, pp. 117-126, Feb. 2016.

[13] W. Hu, C. Su, and Z. Chen *et al.*, "Optimal operation of plug-in electric vehicles in power systems with high wind power penetrations," *IEEE Trans. Sustain. Energy*, vol. 4, no. 3, pp. 577–585, Jul. 2013.

[14] F. Kennel, D. Görges, and S. Liu, "Energy management for smart grids with electric vehicles based on hierarchical MPC," *IEEE Trans. Ind. Informat.*, vol. 9, no. 3, pp. 1528-1537, Aug. 2013.

[15] H. Yang, C. Y. Chung, and J. Zhao, "Application of plug-in electric vehicles to frequency regulation based on distributed signal acquisition via limited communication," *IEEE Trans. Power Syst.*, vol. 28, no. 2, pp. 1017-1026, May 2013.

[16] K. Wang, L. Gu, and X. He, *et al.* "Distributed energy management for vehicle-to-grid networks," *IEEE Network,* vol. 31, no. 2, Mar. 2017, pp. 22-28, Mar. 2017.

[17] V. Güngör, D. Sahin, and T. Kocak, *et al.,* "Smart grid technologies: communication technologies and standards," *IEEE Trans. Ind. Informat.*, vol. 7, no. 4, pp. 529-539, Nov. 2011.

[18] C. Quinn, D. Zimmerle, and T. H. Bradley, "The effect of communication architecture on the availability, reliability, and economics of plug-in hybrid electric vehicle-to-grid ancillary services," *J. Power Sources,* vol. 195, no. 5, pp. 1500-1509, Aug. 2010.

[19] Q. Dong, D. Niyato, and P. Wang, *et al.* "The PHEV charging scheduling and power supply optimization for charging stations," *IEEE Trans. Veh. Technol.*, vol. 65, no. 2, pp. 566-580, Feb. 2016.

[20] A. Mahmood, N. Javaid, and S. Razzaq, "A review of wireless communications for smart grid," *Renew. Sustain. Energy Rev.*, vol. 41, pp. 248-260, Sep. 2015.

[21] H. Su, M. Qiu, and H. Wang, "Secure wireless communication system for smart grid with rechargeable electric vehicles," *IEEE Commun. Mag.,* vol. 50, no. 8, Aug. 2012.

[22] Q. Li, Z. Feng, and W. Li, *et al.* "Joint spatial and temporal spectrum sharing for demand response management in cognitive radio enabled smart grid," *IEEE Trans. Smart Grid,* vol. 5, no. 4, pp. 1993-2001, Jul. 2014.

[23] R. Yu, Y. Zhang, and S. Gjessing, *et al.,* "Cognitive radio based hierarchical communications infrastructure for smart grid," *IEEE Network,* vol. 25, no. 5, pp. 6-14, Oct. 2011.

[24] K. Ko and D. Sung, "The effect of cellular network-based communication delays in an EV aggregator's domain on frequency regulation service," *IEEE Trans. Smart Grid*, vol. 10, no. 1, pp. 65–73, Jan. 2019.

[25] V. C. Gungor and D. Sahin, "Cognitive radio networks for smart grid applications: A promising technology to overcome spectrum inefficiency," *IEEE Veh. Technol. Mag.*, vol. 7, no. 2, pp. 41-46, Apr. 2012.

[26] "Report of the Spectrum Efficiency Working Group, Federal Communications Commission," Spectrum Policy Task Force, Tech. Rep., 2002.

[27] Q. Dong, D. Niyato, and P. Wang, "Dynamic spectrum access for meter data transmission in smart grid: Analysis of packet loss," *in Proc. IEEE WCNC,* pp. 1817-1822, Apr. 1-4, 2012.

[28] A. U. Rehman, C. Dong, and L. L. Yang, *et al.* "Performance of cognitive stop-and-wait hybrid automatic repeat request in the face of imperfect sensing," *IEEE Access*, vol. 4, pp. 5489-5508, Jul. 2016.

[29] B. Zhou, X. Liu, and Y. Cao, *et al.* "Optimal scheduling of virtual power plant with battery degradation cost," *IET Gener. Transm. Distrib.,* vol. 10, no. 3, pp. 712-725, Feb. 2016.

[30] K. Ko and D. Sung, "The effect of EV aggregators with time-varying delays on the stability of a load frequency control system," *IEEE Trans. Power Syst.*, vol. 33, no. 1, pp. 699-680, Jan. 2018.

[31] C. Yang, J. Yao, and W. Lou, *et al.* "On demand response management performance optimization for microgrids under imperfect communication constraints," *IEEE Internet Things J.*, vol. 4, no. 4, pp. 881-893, Aug. 2017.

[32] P. Pinson, G. Papaefthymiou and B. Klockl, *et al.* "From probabilistic forecasts to statistical scenarios of short-term wind power production," *Wind Energy*, vol. 12, no. 1, pp. 51-62, 2009.

[33] S. Weisberg, *Applied linear regression*. Hoboken, NJ, USA: John Wiley & Sons, 2005.

[34] Y. Guo, J. Xiong and S. Xu, *et al.* "Two-stage economic operation of microgrid-like electric vehicle parking deck," *IEEE Trans. Smart Grid,* vol. 7, no. 3, pp. 1703-1712, May 2016.

[35] D. Wu, H. Zeng, and C. Lu, *et al.* "Two-stage energy management for office buildings with workplace EV charging and renewable energy," *IEEE Trans. Transport. Electrific.*, vol. 3, no. 1, pp. 225-237, Mar. 2017.

[36] S. Rezaee, E. Farjah, and B. Khorramdel, "Probabilistic analysis of plug-in electric vehicles impact on electrical grid through homes and parking lots," *IEEE Trans. Sustain. Energy*, vol. 4, no. 4, pp. 1024-1033, Oct. 2013.

[37] C. W. Wang and L. C. Wang, "Modeling and analysis for proactive decision spectrum handoff in cognitive radio networks," in *Proc. IEEE ICC,* Jun. 2009, pp. 1–6.

[38] J. Löfberg, "YALMIP: A toolbox for modeling and optimization in MATLAB," in *Proc. CACSD Conf.*, 2004, pp. 284-289.

[39] X. Liu, "Economic load dispatch constrained by wind power availability: a wait-and-see approach," *IEEE Trans. Smart Grid*, vol. 1, no. 3, pp. 347-355, Dec. 2010.
[40] J. Morales, A. Conejo, and J. Pérez-Ruiz, "Short-term trading for a wind power producer," *IEEE Trans. Power Syst.*, vol. 25, no. 1, pp. 554-564, Feb. 2010.
[41] S. Pal, and R. Kumar, "Electric vehicle scheduling strategy in residential demand response programs with neighbor connection," *IEEE Trans. Ind. Informat.*, vol. 14, no. 3, pp. 980-988, Mar. 2018.
[42] F. Luo, Z. Dong, and K. Meng, *et al.* "Short-term operational planning framework for virtual power plants with high renewable penetrations," *IET Renew. Power. Gen.*, vol. 10, no. 5, pp. 623-633, Feb. 2016.
[43] Q. Wang, B. Jiang, and B. Li, *et al.*, "A critical review of thermal management models and solutions of lithium-ion batteries for the development of pure electric vehicles," *Renew. Sustain. Energy Rev.*, vol. 64, pp. 106-128, Dec. 2016.
[44] A. Santos, N. McGuckin, and H. Y. Nakamoto, *et al.* "Summary of Travel Trends: 2009 National Household Travel Survey," U.S. Department of Transportation Federal Highway Administration, Washington, DC, USA, Rep. FHWA-PL-11022, Jun. 2011.
[45] NREL, System Advisor Model (SAM). Accessed on Jan. 2017. [Online]. Available: https://sam.nrel.gov
[46] A. Botterud, Z. Zhou, and J. Wang, *et al.*, "Use of Wind Power Forecasting in Operational Decisions," Argonne National Lab., Sep. 2011, Tech. Rep. [Online]. Available: http://www.dis.anl.gov/pubs/71389.pdf
[47] UKPX Auction Historical Data. Accessed on Jan. 2017. [Online]. Available: http://www.apxgroup.com/market-results/apx-power-uk/ukpx-auction-historical-data
[48] J. Dupacova, N. Gröwe-Kuska, and W. Römisch, "Scenario reduction in stochastic programming," *Mathematical Programming*, vol. 95, no. 2, pp. 493-511, Feb. 2003.
[49] L. Cao and H. Zheng, "Distributed rule-regulated spectrum sharing," *IEEE J. Sel. Area. Comm.*, vol. 26, no. 1, pp. 130-145, Jan. 2008.
[50] D. Xu, B. Zhou and K. W. Chan, *et al.*, "Distributed multienergy coordination of multimicrogrids with biogas-solar-wind renewables," *IEEE Trans. Ind. Informat.*, vol. 15, no. 6, pp. 3254-3266, Jun. 2019.

Bin Zhou (S'11-M'13-SM'17) received the B.Sc. degree in electrical engineering from Zhengzhou University, Zhengzhou, China, in 2006, the M.S. degree in electrical engineering from South China University of Technology, Guangzhou, China, in 2009, and the Ph.D. degree from The Hong Kong Polytechnic University, Hong Kong, in 2013. Afterwards, he worked as a Research Associate and subsequently a Postdoctoral Fellow in the Department of Electrical Engineering of The Hong Kong Polytechnic University. Now, he is an Associate Professor in the College of Electrical and Information Engineering, Hunan University, Changsha, China. His main fields of research include smart grid operation and planning, renewable energy generation, and energy efficiency.

Kuan Zhang received the B.Sc. degree in electrical engineering from Hainan University, Haikou, China, in 2017. He is currently pursuing the Ph.D. degree at the College of Electrical and Information Engineering in Hunan University, Changsha, China. His major research interests include integrated energy system operation and optimization, renewable energy generation.

Ka Wing Chan (M'98) received the B.Sc. (with First Class Honors) and Ph.D. degrees in electronic and electrical engineering from the University of Bath, Bath, U.K., in 1988 and 1992, respectively. He currently is an Associate Head and Associate Professor in the Department of Electrical Engineering of The Hong Kong Polytechnic University. His general research interests include smart grid and renewable energy, power system stability analysis and control, power system planning and optimization, real-time power system simulation.

Canbing Li (M'06-SM'13) received the B.Sc. degree and the Ph.D. degree both in electrical engineering from Tsinghua University, Beijing, China, in 2001 and 2006, respectively. He is currently a Professor with the College of Electrical and Information Engineering, Hunan University, Changsha, China. His research interests include smart grid, energy efficiency and energy policy.

Xi Lu received the B.Sc. degree in electrical engineering from the North China Electric Power University, Beijing, China, in 2015. He is currently working toward the Ph.D. degree in electrical engineering at the Hong Kong Polytechnic University, Hong Kong. His research interests include the application of robust optimization and distributionally robust optimization in power system operation.

Siqi Bu (S'11–M'12–SM'17) received the Ph.D. degree in electric power and energy research cluster from the Queen's University of Belfast, Belfast, U.K., in 2012, where he continued his postdoctoral research work before entering industry. He was with National Grid U.K. as an Experienced U.K. National Transmission System Planner and Operator. He is currently an Assistant Professor with The Hong Kong Polytechnic University, Hong Kong, and a Chartered Engineer with the U.K. Royal Engineering Council, London, U.K. His research interests include power system stability analysis and operation control, including wind power generation, PEV, HVDC, FACTS, ESS, and VSG.

Xiang Gao is currently working toward the Ph.D. degree in electrical engineering at the Hong Kong Polytechnic University, Hong Kong. Her research interests include renewable energy resources, stochastic optimization and electricity market.